

Oxidation of Aqueous Polyselenide Solutions. A Mechanistic Pulse Radiolysis Study

Andreas Goldbach

University of Stuttgart, Nobelstrasse 12, D-70569 Stuttgart, Germany

Marie-Louise Saboungi* and J. A. Johnson

Argonne National Laboratory, Argonne, Illinois 60439

Andrew R. Cook

Chemistry Department, Brookhaven National Laboratory, Upton, New York 11973

Dan Meisel

Radiation Laboratory and Department of Chemistry and Biochemistry, University of Notre Dame, Notre Dame, Indiana 46556

Received: December 10, 1999; In Final Form: February 17, 2000

The oxidation of aqueous polyselenide solutions was studied by pulse radiolysis in the presence of N₂O at pH 12.3; the hydroxyl radical OH was the predominant oxidant, while hydrogen selenide anions HSe⁻ and triselenide dianions Se₃²⁻ were the major selenide species in the starting solution. The progress of the oxidation was monitored by optical spectroscopy. Transient polyselenides appeared immediately after the electron pulse and rapidly proceeded to form adducts with HSe⁻, i.e., HSe₂²⁻ and H₂Se₂⁻, and a fairly long-lived intermediate that was identified as the diselenide radical anion Se₂⁻. These radicals recombine to give eventually the tetraselenide dianion, Se₄²⁻.

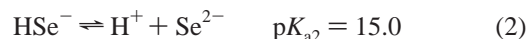
Introduction

Polyselenides are a frequently encountered but relatively little studied species. They are particularly common in high efficiency photoelectrochemical cells using II–VI compounds (often CdSe or GaAs) as anodes, where a selenide salt is added to the electrolyte to minimize anodic photocorrosion.¹ The photo-generated holes react with the selenide ions generated at the solid/liquid interface to produce selenide radicals, which eventually produce polyselenides.² Investigation of the chemistry and dynamics of the polyselenides will provide important information on their stability in different media and thus enable a better control of the factors governing the longevity and performance of the cells. At present, not much is known about the properties and nature of the various species involved in the formation of polyselenides in aqueous solution.^{3,4} The purpose of the experimental work presented here is to fill this gap.

The absorption spectra of aqueous polyselenides have been measured.^{5,6} It was recognized that complex equilibria exist between the various dianions Se_x²⁻, where $x = 1-4$, and some of the equilibrium constants were determined.⁶ The corresponding redox potentials were obtained by potentiometric measurements.⁵ A recent electrospray mass spectroscopy study⁷ revealed that protonated species HSe_x⁻ exist in these electrolyte solutions as well and even larger dianions such as Se₅²⁻ were also identified. However, Lyons and Young detected no paramagnetic species in these solutions using ESR spectroscopy.⁵ An early pulse radiolysis investigation of H₂Se solutions is the only study focusing on polyselenide radicals in aqueous environments.⁸ In this pioneering work Se⁻, its protonated form HSe, and the adduct to HSe⁻, i.e., H₂Se₂⁻, were identified and equilibria and rate constants for some reactions of these radicals were

determined. Only recently have we obtained evidence for the formation of Se₂⁻ radical anions in aqueous polyselenide electrolytes.⁹

The makeup of polyselenide electrolytes is very complicated even in the absence of radicals: the diverse equilibria between the Se_x²⁻ dianions and the protonated HSe_x⁻ depend strongly on the mean oxidation state of the electrolyte, the pH, and the counterion.⁵⁻⁷ However, the dissociation constants K_a of H₂Se¹⁰⁻¹² and H₂Se₂⁸ are well established. The pK_a values of both molecules are the following:



At pH 12.3, employed in this study, equilibrium 2 is completely shifted to the left side.¹² Hence, Se²⁻ does not play a role at all and fully reduced Se appears only as the monoprotonated HSe⁻. On the other hand, the dissociation constants of H₂Se₂ are significantly larger than those of the parent molecule, H₂Se, and equilibrium 4 is completely shifted to the right side. Thus, the diselenide dianion is fully deprotonated at the pH relevant to this study.⁸ Following this trend, and the well-established correlation of pK_a 's with the electrostatic proton–base interactions, the pK_a values of the higher polyselenides are assumed to be similar to those of H₂Se₂ or even smaller. Therefore, we

TABLE 1: Combination of Stock Solutions To Yield the Polyselenide Solutions Used in the Present Study

conv ratio (Se ⁰ /Se ²⁻)	Se oxidation level (%)	0.084 M H ₂ Se (mL) ^a	0.01 M H ₂ O ₂ (mL) ^b	0.1 M NaOH (mL) ^b	H ₂ O (mL) ^b
0	0	5	0	20	75
0.14	12	10	10	40	140
0.91	48	15	60	60	165

^a Deaerated with argon. ^b Deaerated with N₂O.

conclude that at pH > 12 the larger polyselenides are also fully deprotonated.

In the course of Raman spectroscopic studies we observed the formation of Se₂⁻ in aqueous polyselenide solutions following excitation with blue or green laser light.⁹ The radical was identified by its characteristic Raman band at 324 cm⁻¹. Se₄²⁻ was the only other polyselenide detected by means of Raman spectroscopy in that study. Hence, we speculated that the photolysis of Se₄²⁻ leads to homolytic dissociation of the molecule. In the present pulse radiolysis investigation we prepare radicals by a well-defined route and study the oxidation processes and the evolution of polyselenide species. One electron oxidation of polyselenides was achieved using hydroxyl radicals, which were generated by an electron pulse in the presence of N₂O. Optical spectroscopy was used to identify transient species and end products, and a mechanism was devised for the oxidation of selenide in aqueous solution.

Experimental Section

Preparation of Polyselenide Solutions. H₂O₂ was used for partial oxidation of H₂Se in alkaline solutions because it provides controlled and reproducible conversion of selenide into polyselenide. Appropriate quantities of aqueous stock solutions of H₂Se, H₂O₂, and NaOH were mixed in water to yield the polyselenide at the proper pH. All stock solutions were freshly prepared in a glovebox under nitrogen atmosphere prior to each preparation of the polyselenides. Water, 0.1 M NaOH, and 0.01 M H₂O₂ were deoxygenated by bubbling N₂O for 15–20 min in a septum-sealed flask. Saturated H₂Se solutions (8.4 × 10⁻² M at 28 °C)¹³ were prepared in the same way by bubbling the gas into water that was previously deaerated with argon. All chemicals were of the highest purity commercially available, and Nanopure water from a Barnstead Ultrapure water system was used throughout.

Following the procedure described above, sodium selenide solutions were produced at a total Se concentration of 4.2 × 10⁻³ M at pH = 12.3 with 0%, 12%, and 48% of the Se formally oxidized to Se⁰. Details are given in Table 1. Nominally, a 50% oxidation level corresponds to 100% conversion to Se₂²⁻; however, higher oxidized polyselenides, such as Se₃²⁻ or Se₄²⁻, may form as well, via the equilibria between these species in water.^{5–7} Absorption spectra of the solutions were recorded on a Varian Cary 5 spectrophotometer prior to the radiolysis experiments. We limited the selenide conversion in order to avoid complications caused by high oxidation levels, notably the generation of colloidal selenium.

Pulse Radiolysis Experiments. All solutions, degassed with ultrapure argon or N₂O, were manipulated using the syringe technique. Electron pulses of 4–40 ns width from the Argonne 20 MeV electron linear accelerator were used to produce 1.2 × 10⁻⁶ to 2.5 × 10⁻⁵ M hydrated electrons. Measurements were made using 1 cm Suprasil cells and a pulsed xenon lamp was employed as analyzing light source. An N₂O saturated solution of 10⁻² M KSCN was used for dosimetry. The radiolysis of

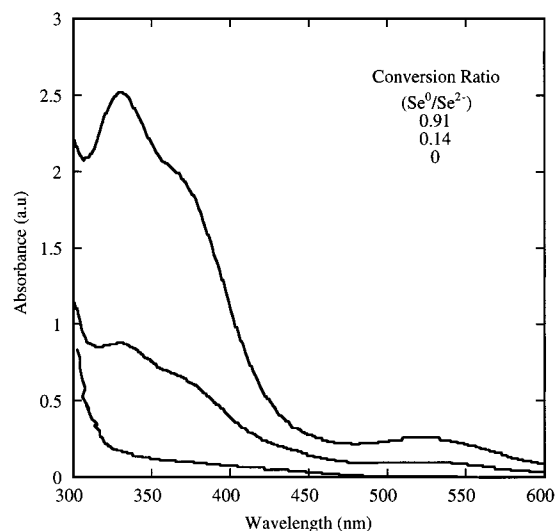


Figure 1. Optical spectra of the polyselenide electrolytes used in the present study. The degree of oxidation increases from the bottom to the top. Experimental conditions: [OH⁻] = 1.75 × 10⁻² M, [H₂Se]₀ = 4.2 × 10⁻³ M.

water generates e_{aq}⁻ and OH radicals as the primary products at a yield of 2.8 radicals per 100 eV each. Other minor products, H and H₂O₂, were neglected. When the solutions contain N₂O, all the e_{aq}⁻ are converted to OH radicals via the reaction



Thus, the OH concentration is 5 × 10⁻⁵ M at the maximum radiation dose used. Because of the high pH, some of these radicals may dissociate to their basic form, the O⁻ radicals (pK_a = 11.9). The latter are expected to react slower than the OH radicals, and therefore most of the reaction would proceed via oxidation by OH coupled to its acid–base equilibrium. N₂O concentrations were slightly below the saturation level at 1 atm (2.0 × 10⁻² M at 25 °C)¹⁴ because of the addition of argon-saturated H₂Se solution to the other solutions.

Results

The absorption spectra of the polyselenide solutions used in the pulse radiolysis experiments are shown in Figure 1. As discussed above, HSe⁻ is the only species expected in the solution prior to oxidation at pH 12.3. The hydrogen selenide anion has a broad absorption band at around 250 nm. Upon oxidation by hydrogen peroxide three bands appear at 330, 380, and 530 nm, as can be seen in Figure 1. These bands indicate the formation of Se₃²⁻, the triselenide dianion.^{5,6} For comparison, the Se₄²⁻ anion has absorption bands at 380 and 470 nm and Se₂²⁻ at 430 nm.^{5,6} Using the spectral parameters derived by Lyons and Young⁵ the best fit to these spectra was obtained with a mixture of 5% of Se₂²⁻ and 95% of Se₃²⁻. Apart from their intensity, the absorption spectra of the two oxidized H₂Se solutions were identical. The predominance of the triselenide even at the lower Se oxidation level is consistent with the electrospray mass spectroscopy study by Raymond et al., who investigated the pH dependence of the polyselenide equilibria in an aqueous Na₂Se₄ solution. They showed that at pH 7 and below almost equal amounts of Se₂²⁻, Se₃²⁻, and Se₄²⁻ coexist in that highly oxidized polyselenide solution (75% conversion to “Se⁰”). Upon raising the pH the concentrations of Se₂²⁻ and Se₃²⁻ decrease and the tetraselenide is clearly favored above pH 11. The predominance of the triselenide at the low

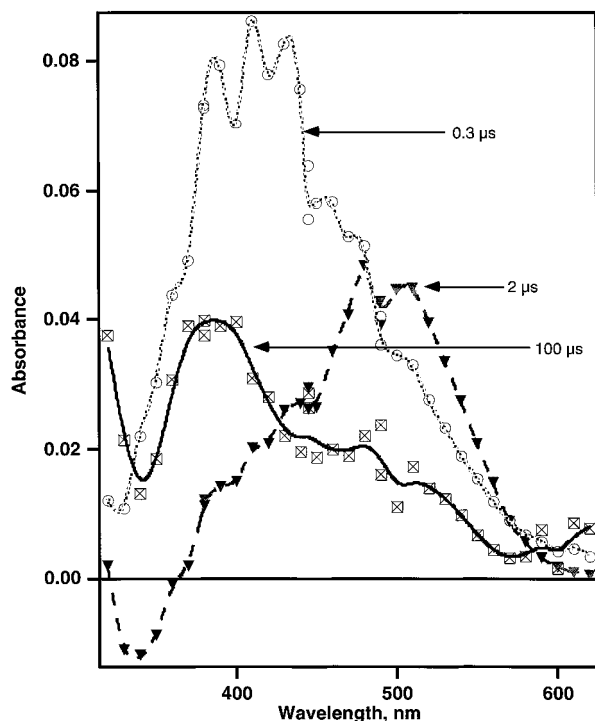


Figure 2. Difference absorption spectra obtained at various times following a pulse that generates 5×10^{-5} M of OH radicals in the solution with an initial Se conversion ratio of 0.14 at pH 12.3. Initial conditions: $[\text{HSe}^-] = 3.45 \times 10^{-3}$ M, $[\text{Se}_3^{2-}]_0 = 2.5 \times 10^{-4}$ M, N_2O saturated solutions.

conversion ratios in the two solutions prepared for the present radiolysis experiments is in line with those observations.

The spectral changes induced by the radiolysis experiments are shown in Figures 2 and 3 (lower and higher initial Se oxidation levels, respectively). *These spectra are difference spectra between the irradiated and the starting polyselenide electrolytes.* Within the first microsecond after the electron pulse, new spectral features emerge and vanish very fast, mainly around 400 nm. At 2 μs after the pulse, both solutions give rather similar absorption spectra with a broad absorption band near 500 nm, a shoulder at around 400 nm, and bleaching of the parent molecule band around 340 nm. These bands further disappear, and at 100 μs after the pulse, the difference absorption spectrum of the highly oxidized electrolyte (Figure 3) shows only a prominent band at 380 nm and a shoulder at 470 nm. In addition to these bands, the less oxidized electrolyte exhibits two more bands at 430 and 520 nm after 100 μs (Figure 2).

Identification of the polyselenide intermediates from these spectra is difficult because of the limited number of well-established optical spectra of reactive polyselenides. The radical anion Se_2^- is best characterized among these since it can be easily implanted into ultramarines,¹⁵ zeolites,¹⁶ and halogenide crystals.¹⁷ It has two characteristic absorption bands in the green and the UV spectral region. For instance, these bands are found at 345 and 515 nm in KI crystals doped with Se_2^- .¹⁷ An absorption band centered at 450 nm has been attributed to Se^- in the pulse radiolysis study of H_2Se solutions.⁸ Other bands were assigned to the radicals HSe (350 nm) and H_2Se_2^- (410 nm). We have no knowledge of any absorption spectra of other selenide radicals in aqueous milieu. The assignment of the difference absorption spectra in Figures 2 and 3 is further complicated by the fact that most of the absorption bands of the reactive intermediates and dianions Se_x^{2-} overlap below 500 nm.

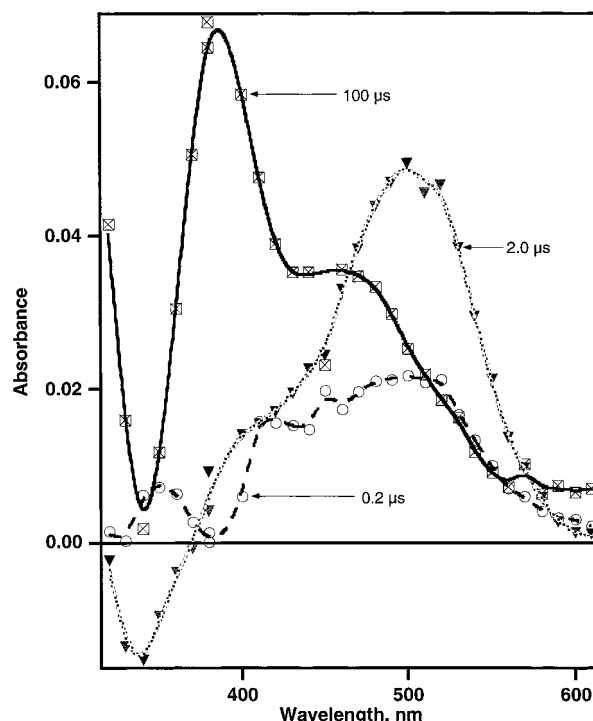


Figure 3. Difference absorption spectra obtained at various times following a pulse that generates 5×10^{-5} M of OH radicals in the solution with an initial Se conversion ratio of 0.91 at pH 12.3. Initial conditions: $[\text{HSe}^-] = 1.2 \times 10^{-3}$ M, $[\text{Se}_3^{2-}]_0 = 1 \times 10^{-3}$ M, N_2O saturated solutions.

Despite these limitations the difference absorption spectra provide several constructive details. First, the bands at 380 and 470 nm in Figure 3 indicate that the tetraselenide Se_4^{2-} is the end product of the radiolytic oxidation on the time scale of our experiments. In the solution with a lower initial Se oxidation level the conversion into Se_4^{2-} is incomplete, as indicated by the additional bands in the 100 μs spectrum of Figure 2. These additional features are attributed to Se_2^{2-} (430 nm) and the intermediate, which dominates the 2 μs spectra with an intense band around 500 nm (Figures 2 and 3). The latter band is centered at 510 nm in Figure 3 and therefore is attributed to Se_2^- . This radical anion appears to be the direct precursor of the tetraselenide, since no other intermediate band is observed en route to Se_4^{2-} . Another notable feature in the 2 μs spectra is the bleaching around 340 nm. In this region Se_3^{2-} dominates the absorption spectrum of the parent polyselenide solution. Hence, the bleaching is attributed to the removal of the triselenide upon reaction with the hydroxyl radicals. Figures 4 and 5 show the temporal evolution of the absorbance at 340 and 510 nm of both solutions, low and high conversions, following the radiation pulse. Significantly, the level of bleaching at 340 nm and the gain in absorbance at 510 nm are equal in both solutions. This indicates that the consumption of Se_3^{2-} and the formation of Se_2^- depend on the radiation dose but not on the initial Se oxidation level of the investigated solutions.

The optical spectrum of Se_4^{2-} displayed in Figure 3 is distorted when compared to that reported by Lyons and Young.⁵ This results from the overlap of the bleached absorption of the parent molecule and that of the oxidation product: The bleached Se_3^{2-} bands and the spectrum of the newly formed Se_4^{2-} blend together to produce the 100 μs spectrum. Indeed, this spectrum can be reproduced satisfactorily by employing the spectral parameters of Se_3^{2-} and Se_4^{2-} determined by Lyons and Young⁵ and assuming the consumption of one Se_3^{2-} per Se_4^{2-} molecule. Also, the level of bleaching at 340 nm after 2 μs translates into

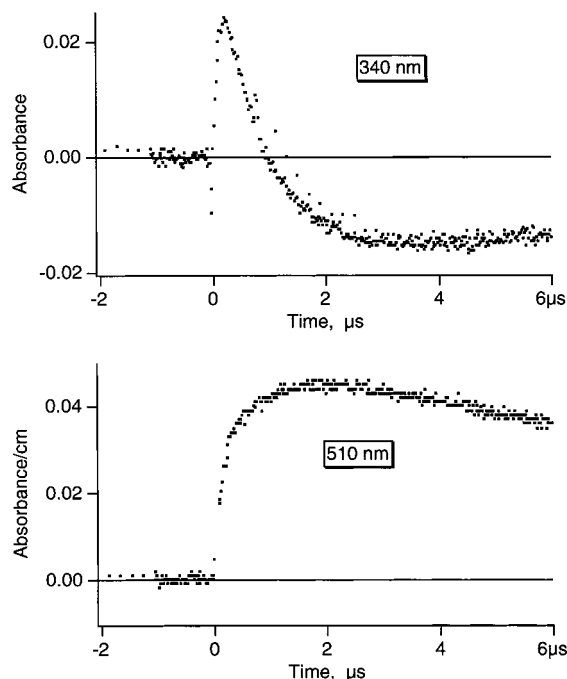


Figure 4. Absorbance changes at 340 and 510 nm of the solution described in Figure 2 at the same radiation dose.

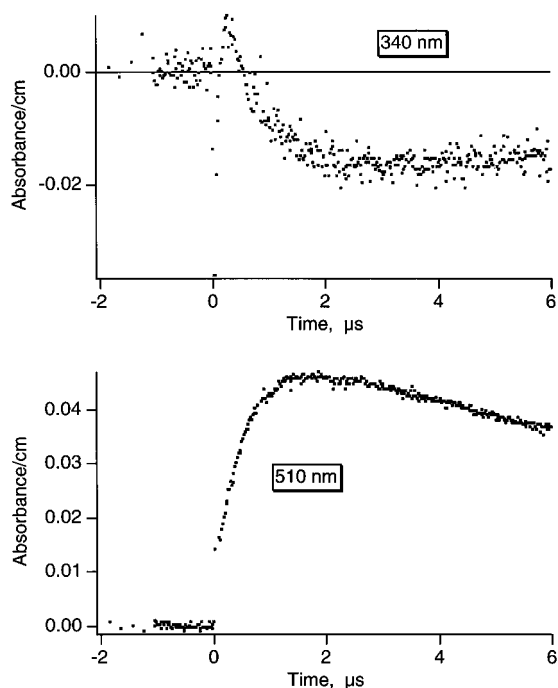


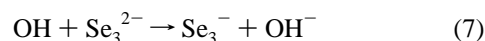
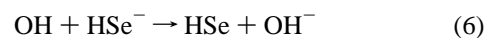
Figure 5. Absorbance changes at 340 and 510 nm of the solution described in Figure 3 at the same radiation dose.

a Se_3^{2-} concentration reduction of 5×10^{-6} M using the extinction coefficient of Se_3^{2-} at this wavelength taken from the investigation of Lyons and Young.⁵ This corresponds to roughly 10% of the expected absorption depletion at the dose used if we assume the consumption of one molecule Se_3^{2-} per OH radical. Clearly, the oxidation products must contribute to the absorption at this wavelength also. Although the absorption at 350 nm in the 0.2 μs spectrum of Figure 3 points to HSe, another species has to be involved because HSe ($\epsilon_{\text{max}} = 300 \text{ M}^{-1} \text{ cm}^{-1}$)⁸ is a much weaker absorber in this spectral range than Se_3^{2-} ($\epsilon_{\text{max}} = 3000 \text{ M}^{-1} \text{ cm}^{-1}$).⁵ It is likely that the hidden band is the second optical transition of the radical Se_2^- , which is found at 345 nm in the KI matrix.¹⁷ The intricacy of the

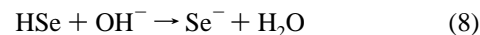
difference spectra makes it very difficult to extract reliable rate constants from the absorbance changes. The intermediate band at 510 nm is the least affected by overlap effects because the optical spectra of Se_3^{2-} and Se_4^{2-} are relatively weak in this spectral range. Notably, the corresponding species Se_2^- disappears in a radiation dose dependent process, which suggests a recombination of these radicals. However, since we do not know the absolute value of the absorption coefficient of Se_2^- at 510 nm, we are unable to determine a rate constant for the recombination.

Discussion

A detailed mechanism can be outlined for the oxidation of polyselenide solutions by OH radicals. The major selenide species in the solutions, prior to the electron pulse, are HSe^- and Se_3^{2-} . One electron oxidation of these selenides by the hydroxyl radicals is the initial step in a sequence that eventually leads to the formation of Se_4^{2-} . The pH used is close to the $\text{p}K_a = 11.9$ of the hydroxyl radical¹⁸ and its corresponding base, O^- , may also participate in the oxidation. The rate constants for reactions of O^- with HSe^- and Se_3^{2-} are expected to be significantly smaller than those of OH, but the OH/ O^- acid-base equilibrium is rapidly achieved on the time scale of the oxidation reactions

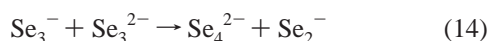
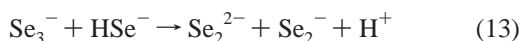
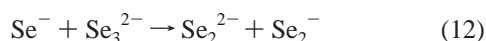
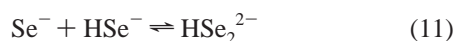
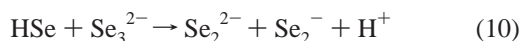


At the lower Se oxidation level the concentrations of Se_3^{2-} and HSe^- are 2.5×10^{-4} and 3.45×10^{-3} M, respectively, and reaction 7 cannot compete with reaction 6 provided that the rate constants are similar. At the higher Se conversion level the concentrations of both Se_3^{2-} and HSe^- are approximately 10^{-3} M and both oxidation routes may be important. The reaction of OH with HSe^- was investigated by Henglein and co-workers and the rate constant for reaction 6 has been determined as $k_6 = 5.5 \times 10^9 \text{ M}^{-1} \text{ s}^{-1}$.⁸ Note that the 350 nm band of HSe can be recognized in the 0.2 μs spectrum of Figure 3. It is much weaker than those of Se_3^{2-} in this spectral range and is masked in the difference absorption spectra when significant amounts of Se_3^{2-} are depleted (2 μs spectra, Figures 2 and 3). The oxidation of Se_3^{2-} by OH has not been studied, and the absorption spectrum of the one electron oxidation product Se_3^- is not known either. Note, however, that the $\text{p}K_a$ of HSe



is expected to be considerably smaller than that of the hydroxyl radical. Therefore, HSe should be mostly ionized at pH 12.3 at equilibrium. The 450 nm absorption due to Se^- ($\epsilon_{\text{max}} = 380 \text{ M}^{-1} \text{ cm}^{-1}$)⁸ is responsible for some of the bands in the 0.2 and 2 μs spectra of Figures 2 and 3.

The primary oxidation products HSe, Se^- , and Se_3^- are rapidly removed by subsequent reactions. HSe has to be considered as well because it may be intercepted by another reactant before it equilibrates according to eq 8. The initial concentration of OH sets an upper limit for the total yield of these intermediates, which is 5×10^{-5} M following the most intense radiation pulse. Because of the much larger concentration of HSe^- and Se_3^{2-} , the reactions that follow the initial oxidation step involve these species:

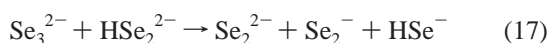
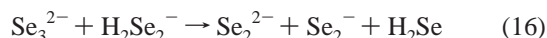


With the exception of the equilibria 9 and 11 these reactions yield a stable polyselenide dianion and the dimeric radical Se_2^- , which was postulated above as an intermediate based on the 2 μs difference absorption spectra. The adducts defined by the equilibria 9 and 11 lead eventually to Se_2^{2-} and Se_2^- also (vide infra). Equilibrium 9 was studied by Henglein and co-workers.⁸ They determined the equilibrium constant $K_9 = 1.7 \times 10^4 \text{ M}^{-1}$ and the absorption spectrum of the complex H_2Se_2^- shows an absorption band centered at 410 nm ($\epsilon_{\text{max}} = 8600 \text{ M}^{-1} \text{ cm}^{-1}$).⁸ Equilibrium 9 is strongly pH dependent and at pH > 12 the 410 nm band is very weak,⁸ suggesting that this complex is of minor importance at very high pH values. Nonetheless, this band may contribute to the absorption around 400 nm in the 0.2 and 2 μs spectra of Figures 2 and 3. No information is available on equilibrium 11 or the spectral characteristics of the complex HSe_2^{2-} . However, it is tied to H_2Se_2^- via the acid–base equilibrium:



where the doubly ionized species, HSe_2^{2-} , is expected to dominate at the pH value of this study.

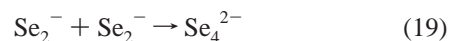
The adducts to selenide stabilize the primary oxidation products, HSe and Se^- , and act as a reservoir for these radicals. As these species are consumed via reactions 10 and 12, equilibria 9, 11, and 15 are shifted to the left side, feeding the restored primary radicals into the consuming reaction channels 10 and 12. Of course, it is possible that the adducts themselves react with Se_3^{2-} , but these routes yield the same products Se_2^{2-} and Se_2^- as reactions 10 and 12:



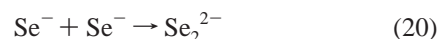
The bleaching level at 340 nm depends on the radiation dose but not on the initial Se oxidation level. The sequence of reactions 6–17 is, in particular, consistent with that observation. In this mechanism the primary oxidation of Se_3^{2-} by OH (eq 7) is important only in the solution with high initial Se conversion. Nonetheless, in the mechanism outlined above, the formation of Se_2^{2-} and Se_2^- consumes exactly one Se_3^{2-} and one HSe^- molecule regardless of the primary oxidation step. Primary oxidation of HSe^- by OH radicals (reactions 6 and 8) is followed by (i) 10 and 12, respectively, or (ii) the detour via the adduct to the parent selenide (reactions 9, 11, and 15) followed by reaction with the parent trimer (reactions 10, 12, 16, and 17, respectively). On the other hand, the sequence that is initiated by the oxidation of the trimer Se_3^{2-} (reaction 7) is followed by a reaction with the parent selenide HSe^- (reaction 13). Either of these sequences leads to the same net reaction:



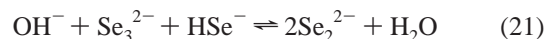
Reaction 14 leads to an increase in the polyselenide chain length, i.e., the formation of Se_4^{2-} from two Se_3^{2-} parent molecules. This pathway seems to be of minor importance in the scheme outlined above. However, the reactive paramagnetic species, Se_2^- , which results from any of the pathways shown above, eventually recombines to yield the Se_4^{2-} . This is evident from the dose dependent decay of the absorbance at 510 nm:



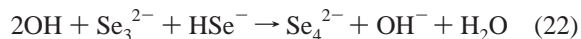
Since the absorption coefficient of Se_2^- at 510 nm is not known, we are unable to determine the rate constant $2k_{19}$ of the recombination. However, it is expected to be of the same order as the rate constant found for the recombination of Se^- :



where $2k_{20} = 4.6 \times 10^9 \text{ M}^{-1} \text{ s}^{-1}$.⁸ According to eqs 18 and 19 two molecules of Se_3^{2-} are consumed in the formation of Se_4^{2-} . However, the 100 μs spectrum of Figure 3 implies the loss of just one Se_3^{2-} molecule in this process and it does not indicate the formation of two Se_2^{2-} as byproduct either. Nonetheless, the interim formation of Se_2^{2-} is supported by the 430 nm band in the 100 μs spectrum of Figure 2. Notably, the Se_2^{2-} band is accompanied by the 510 nm band of Se_2^- and the 380 and 470 nm bands of Se_4^{2-} in Figure 2, which suggests that the formation of Se_4^{2-} is considerably slower in the solution with the lower initial Se oxidation level. Here the HSe/Se^- reservoir character of the equilibria 9, 11, and 15 becomes evident. Since the concentration of HSe^- exceeds that of Se_3^{2-} by more than an order of magnitude in this solution, most of the primary radicals are captured by HSe^- . The release of HSe/Se^- radicals by the Equilibria 9, 11, and 15 then becomes the step controlling the overall rate. Note that these “reservoir” species, (HSe_2^{2-} and H_2Se_2^-) retard the depletion of Se_3^{2-} , which contributes to the relatively weak bleaching at 340 nm. Finally, the absence of 430 nm bands in the 100 μs spectrum of Figure 3 and the “missing” Se_3^{2-} molecule can be rationalized by taking the following equilibrium into account:



The electrospray mass spectroscopy study of Raymond et al.⁷ showed that at pH > 7 this equilibrium is strongly shifted to the left. So, one molecule Se_3^{2-} is recovered while the Se_2^{2-} is completely consumed and the stoichiometric combination of eqs 18, 19, and 21 gives the overall equation for the selenide oxidation triggered by the radiolysis pulse:



Equation 22 is also consistent with other Se_4^{2-} delivering reactions, such as the direct association of Se^- and Se_3^- produced in eqs 6 and 7 or reaction 20. However, because the concentrations of the short-lived radicals are much smaller than those of the parent molecules, HSe^- and Se_3^{2-} , intervention by the latter dominates. Whereas this study focuses on the oxidation of Se_3^{2-} , the results are of general importance for the understanding of aqueous polyselenides. First, Se_2^- is evidently a key species in the redox chemistry of polyselenides. Its formation favors the conversion to Se_4^{2-} . Other Se_x^{2-} dianions that may be thermodynamically favored form subsequently according to the established polyselenide equilibria.^{5–7} Second,

the adduct radicals $\text{H}_2\text{Se}_2^-/\text{HSe}_2^{2-}$ become of crucial importance. They serve as a reservoir for the primary radical, HSe/Se^- , and the release of that radical from the adduct may control the overall rate.

Conclusion

The oxidation of aqueous polyselenide electrolytes has been studied by pulse radiolysis experiments on N_2O saturated solutions so that the hydroxyl radical OH was the main oxidizing agent. The electrolytes were characterized by optical spectroscopy. The hydrogen selenide anion HSe^- and the triselenide dianion Se_3^{2-} were the major selenide species in the solutions prior to the radiolysis. We have drawn up an oxidation mechanism that accounts for all the crucial details of the difference absorbance spectra, i.e., (i) the depletion of Se_3^{2-} , (ii) the intermediate with an absorption band at 510 nm, (iii) the end product Se_4^{2-} , (iv) the interim product Se_2^{2-} , (v) the depletion of 1 mol of Se_3^{2-} per Se_4^{2-} , and (vi) the formation of Se_4^{2-} via recombination of the intermediate. After the electron pulse HSe , Se^- , and probably Se_3^- form, but these are short-lived and soon the optical spectra are dominated by an optical band around 500 nm, which is attributed to the Se_2^- . This radical anion is fairly stable on the time scale of our experiments and eventually proceeds to form the tetraselenide Se_4^{2-} via recombination. In addition, we have evidence for the existence of reservoir species H_2Se_2^- and HSe_2^{2-} that stabilize the primary HSe and Se^- radicals temporarily. The release of HSe or Se^- from these HSe^- adducts is the rate-controlling step in electrolytes with low initial oxidation level.

Acknowledgment. The work at ANL is supported by the U.S. Department of Energy, Division of Materials Sciences,

Office of Basic Energy Sciences, under Contract No. W-31-109-ENG-38. A.G. gratefully acknowledges support by the Deutsche Forschungsgemeinschaft. Work at BNL and NDRL is supported by the US-DOE, Division of Chemical Sciences. This is document NDRL No. 4139.

References and Notes

- (1) Licht, S. *Sol. Energy Mater. Sol. Cells* **1995**, *38*, 305.
- (2) Dimitrijevic, N. M.; Kamat, P. V. *Langmuir* **1987**, *3*, 1004.
- (3) Kanatzidis, M. G. *Comments Inorg. Chem.* **1990**, *10*, 161.
- (4) Ansari, M. A.; Ibers, J. A. *Coord. Chem. Rev.* **1990**, *100*, 223.
- (5) Lyons, L. E.; Young, T. L. *Austr. J. Chem.* **1986**, *39*, 511.
- (6) Licht, S.; Forouzan, F. *J. Electrochem. Soc.* **1995**, *142*, 1546.
- (7) Raymond, C. C.; Dick, D. L.; Dorhout, P. K. *Inorg. Chem.* **1997**, *36*, 2678.
- (8) Schöneshöfer, M.; Karmann, W.; Henglein, A. *Int. J. Rad. Phys. Chem.* **1969**, *1*, 407.
- (9) Goldbach, A.; Johnson, J.; Meisel, D.; Curtiss, L. A.; Saboungi, M.-L. *J. Am. Chem. Soc.* **1999**, *121*, 4461.
- (10) Hagiwara, H. *Abstr. Rikwagaku-Kenkyu-Ih* **1941**, *20*, 30.
- (11) Wood, R. H. *J. Am. Chem. Soc.* **1958**, *80*, 1559.
- (12) Levy, D. E.; Myers, R. J. *J. Phys. Chem.* **1990**, *94*, 7842.
- (13) Fogg, P. G. T., Young, C. L., Eds. *Hydrogen Sulfide, Deuterium Sulfide, and Hydrogen Selenide*; IUPAC Solubility Data Series, Vol. 32; Pergamon Press: Oxford, U.K., 1988.
- (14) Young, C. L., Ed. *Oxides of Nitrogen*; IUPAC Solubility Data Series, Vol. 8; Pergamon Press: Oxford, U.K., 1981.
- (15) Clark, R. J. H.; Dines, T. J.; Kurmoo, M. *Inorg. Chem.* **1983**, *22*, 2766.
- (16) Goldbach, A.; Grimsditch, M.; Iton, L.; Saboungi, M.-L. *J. Phys. Chem. B* **1997**, *101*, 330.
- (17) Murata, H.; Kishigami, T.; Kato, R. *J. Phys. Soc. Jpn.* **1990**, *59*, 506.
- (18) Rabani, J.; Matheson, M. *J. Am. Chem. Soc.* **1964**, *86*, 3175.